

LIBRARIES



3 9080 02754 3898

Report 1529



DEPARTMENT OF THE NAVY
DAVID TAYLOR MODEL BASIN

HYDROMECHANICS

A METHOD OF CALCULATING THE SPINDLE TORQUE OF A
CONTROLLABLE-PITCH PROPELLER AT DESIGN CONDITIONS

AERODYNAMICS



by

Robert J. Boswell

STRUCTURAL
MECHANICS

SEP 15 1961



HYDROMECHANICS LABORATORY

RESEARCH AND DEVELOPMENT REPORT

APPLIED
MATHEMATICS

August 1961

Report 1529

A METHOD OF CALCULATING THE SPINDLE TORQUE OF A
CONTROLLABLE-PITCH PROPELLER AT DESIGN CONDITIONS

by

Robert J. Boswell

August 1961

Report 1529
S-R009 01 01

TABLE OF CONTENTS

| | Page |
|--|------|
| ABSTRACT | 1 |
| INTRODUCTION | 1 |
| GENERAL CONSIDERATIONS | 4 |
| PROCEDURE | 6 |
| Hydrodynamic Component of Blade Spindle Torque | 7 |
| Centrifugal Component of Blade Spindle Torque | 12 |
| Changed Location of Spindle Axis | 17 |
| Off-Design Conditions | 18 |
| EXAMPLE | 20 |
| Hydrodynamic Blade Spindle Torque | 22 |
| Centrifugal Blade Spindle Torque | 24 |
| Location of Optimum Spindle Axis | 26 |
| CONCLUDING REMARKS | 28 |
| REFERENCES | 29 |
| APPENDIX - Derivation of Expression for Centrifugal Component of Spindle Torque | 31 |

LIST OF FIGURES

| | Page |
|---|------|
| Figure 1 - Propeller Isometric Showing Hydrodynamic Forces | 8 |
| Figure 2 - Diagram of Hydrodynamic Forces and Distances to Initial Spindle Axis | 9 |
| Figure 3 - Propeller Isometric Showing Centrifugal Forces | 13 |
| Figure 4 - Diagram of Centrifugal Forces and Distances to Initial Spindle Axis | 14 |
| Figure 5 - Effect of Changed Spindle Axis Location on Hydrodynamic Blade Spindle Torque | 16 |
| Figure 6 - Effect of Changed Spindle Axis Location on Centrifugal Blade Spindle Torque | 16 |
| Figure 7 - Drawing of Example Propeller | 21 |
| Figure 8 - Lift Distribution of $a = 0.8$ Mean Line | 21 |
| Figure 9 - Radial Distribution of Hydrodynamic and Centrifugal Components of Blade Spindle Torque for Example Propeller. | 27 |
| Figure 10- Variation of Spindle Torque with Location of Spindle Axis for Example Propeller | 27 |

NOTATION

| | |
|----------------|---|
| A | Cross-sectional area of developed blade section |
| a | Coefficient for calculating area (as used in Reference 11) |
| b | Coefficient for calculating I_{x_0} (as used in Reference 11) |
| C | Nondimensional section length |
| C_c | Percent chord from leading edge to center of pressure |
| C_D | Drag coefficient of blade section |
| C_L | Lift coefficient of blade section |
| C_m | Percent chord from leading edge to point of maximum thickness |
| C_x | Percent chord from leading edge to any point along chord |
| c | Coefficient for calculating I_{y_0} (as used in Reference 11) |
| d(CF) | Centrifugal force on differential element of blade mass |
| dC | Differential distance along chord |
| dm | Differential element of blade mass |
| dx | Nondimensional differential distance along radius |
| dr | Differential distance along radius |
| dy | Differential distance in y - direction |
| dz | Differential distance in z - direction |
| d γ | Differential of angle γ |
| I_{max} | Maximum moment of inertia of blade section about section centroid |
| I_{x_0} | Moment of inertia of blade section about the axis parallel to root-tail line and passing through section centroid (as used in Reference 11) |
| I_{y_0} | Moment of inertia of blade section about the axis perpendicular to root-tail line and passing through section centroid (as used in Reference 11) |
| I_{min} | Minimum moment of inertia of blade section about section centroid |
| I_{yz} | Product of inertia of blade section with respect to axes in plane of section parallel and perpendicular to direction of advance and passing through point of intersection of spindle axis and blade section |
| \bar{I}_{yz} | Product of inertia of blade section with respect to axes through section centroid parallel and perpendicular to direction of advance |
| l | Length of blade section |
| m_x | Maximum camber of meanline |

| | |
|---------|--|
| P_e | Effective horsepower |
| P_s | Shaft horsepower |
| p | Static pressure at point on blade |
| Q_c | Centrifugal component of blade spindle torque, positive in direction towards larger positive pitch settings |
| Q'_c | Differential centrifugal spindle torque due to centrifugal force distribution over blade section |
| Q''_c | Differential centrifugal spindle torque due to centrifugal force on element of blade mass |
| Q_h | Hydrodynamic component of blade spindle torque, positive in direction towards larger positive pitch settings |
| Q'_h | Differential hydrodynamic spindle torque at one blade section |
| q | Free-stream dynamic pressure |
| R | Propeller radius |
| R_a | Offset of section from arbitrary spindle axis due to rake, positive towards downstream of flow |
| r | Radius of any propeller blade section |
| r_h | Radius hub section |
| S_k | Offset of blade section due to skew, offset towards trailing edge positive |
| t | Thrust deduction fraction |
| t_x | Maximum blade section thickness |
| u | Component of distance from spindle axis to any given point on chord in plane normal to propeller axis, positive towards direction of rotation |
| V | Ship velocity |
| V_A | Velocity of advance |
| V_r | Resultant inflow velocity |
| v | Component of distance from spindle axis to any given point on chord in plane of spindle axis and propeller axis, positive towards forward direction of advance |
| w_o | Effective wake fraction |
| w_x | Local wake fraction (circumferential average of axial wake) |
| X_c | Coordinate of section centroid in direction of nose-tail line as measured from half-chord point, positive towards leading edge |
| x | Nondimensional radius, r/R |
| x_h | Nondimensional radius of hub section r_h/R |
| x_l | Coordinate of leading edge of section in direction of nose-tail line as measured from section centroid (as used in Reference 11) |

| | |
|-----------|--|
| Y | Component of distance from spindle axis to any point on blade section as measured along blade section, positive towards direction of rotation |
| \bar{Y} | Component of distance from spindle axis to section centroid in plane normal to propeller axis, positive towards direction of rotation |
| Y_c | Coordinate of section centroid in direction perpendicular to nose-tail line as measured from nose-tail line, positive towards back of section |
| y_1 | Coordinate of leading edge of section in direction perpendicular to nose-tail as measured from section centroid, positive towards back of section (as used in Reference 11) |
| Z | Component of distance from spindle axis to any point on blade section in plane of spindle axis and propeller axis, positive towards forward direction of advance |
| \bar{Z} | Component of distance from spindle axis to section centroid in plane of spindle axis and propeller axis, positive towards forward direction of advance |
| α | Angle of attack at which the section is operating |
| β | Advance angle |
| β_i | Hydrodynamic pitch angle |
| γ | Angular displacement from spindle to any point on blade as measured about propeller axis in a plane normal to the propeller axis, positive towards leading edge |
| S | Rake angle measured from propeller disc, positive after-rake |
| Θ | Arbitrary angle through which spindle axis is rotated |
| ρ | Density of fluid |
| ρ_b | Density of propeller blade |
| ϕ | Pitch angle of the blade section, positive for forward pitch settings |
| ϕ_h | Pitch angle of blade section at the hub, positive for forward pitch settings |
| ω | Angular velocity of propeller (radians/unit time) |

ABSTRACT

A procedure for calculating the spindle torque and for determining the "optimum" spindle axis location of a controllable-pitch propeller at design conditions is presented. From the blade geometry and theoretical pressure distribution the hydrodynamic and centrifugal forces acting on the blade are obtained, and from the distribution of these forces the spindle torque is calculated. The optimum spindle axis location is then determined by an iteration process. An example is included to illustrate the procedure.

INTRODUCTION

A controllable-pitch propeller is defined as a propeller in which the pitch can be changed during propeller operation by turning each blade about a radial or near radial axis. This pitch-changing axis is called the spindle axis. There are two types of forces acting on a propeller blade under operating condition: (1) hydrodynamic forces composed of lifting forces (due to the pressure distribution) and viscous drag forces, and (2) centrifugal forces (due to the rotating blade mass). The distribution of these forces over the blade produces a torque about the spindle axis. This torque is called the spindle torque. It is desirable to have the maximum spindle torque encountered under ordinary operating conditions as small as possible in order to minimize the maximum loads placed upon the pitch-changing mechanism. This report presents an approximate method of locating the spindle axis of any given blade so as to produce zero spindle torque at design conditions and, for controllable-pitch propellers with previously located spindle axes, of calculating the spindle torque at design conditions.

A controllable-pitch propeller is designed by essentially the same procedure as an ordinary fixed-pitch propeller except that the magnitude of the spindle torque must also be taken into consideration. Such design parameters as blade rake, blade skew, blade outline, type of blade section, design pitch distribution, and spindle axis location greatly influence the magnitude of spindle torque. Since the relationships for the variation

of pressure distribution and centrifugal force distribution on a propeller blade over the range of operating conditions (forward, backing, and transient conditions) follow different laws, the hydrodynamic and centrifugal components of the blade spindle torque cannot be made to balance over the entire operating range. However, the parameters can be chosen so as to minimize the largest spindle torque that will be encountered under any operating condition provided the effects of the various parameters upon the magnitude of the spindle torque are known throughout the range of operating conditions and a method of calculating the spindle torque for any condition is available.

Additional compromises, depending upon the application of the propeller, must be made in the propeller design. For harbor tugs, in which backing is an important consideration, some sacrifice of forward performance must be made in order to obtain better backing characteristics. Symmetrical or slightly cambered sections may be employed to obtain a more favorable pressure distribution and better cavitation characteristics under backing conditions. A pitch distribution with reduced pitch at inner sections of the propeller blade at forward pitch settings is necessary to prevent the inner blade sections from having a positive pitch at negative nominal pitch settings. For propellers producing greater speed and power, large compromises in camber and pitch distribution cannot be made without great sacrifice in full speed ahead performance due to cavitation considerations at full speed ahead. The inner sections of the propeller blade must be made thicker than for comparable fixed-pitch propellers due to the unusually high blade loadings encountered under transient conditions during emergency stopping and backing operations.

In order to permit the housing of the pitch-changing mechanism, the hub size must be somewhat large on a controllable-pitch propeller than on a fixed-pitch propeller (hub diameter ratio of order of magnitude of .30 to .35 for a controllable pitch propeller).¹ This larger hub size will cause only a slight loss in maximum propeller efficiency (of order of magnitude of 2 percent or less)¹ provided the hub and blades are properly faired. Due to space limitations near the hub, the number of blades must often be limited to three.²

¹ References are listed on page 29.

There is little quantitative information available on the effects of the various parameters upon spindle torque. Rusetskiy and Favorskaia³ investigated the effect of blade outline and nominal pitch ratio upon the hydrodynamic component of spindle torque at dead pull condition. They developed a relationship whereby section angle of attack is obtained for any pitch setting at dead pull conditions. The section moment coefficient is then obtain from standard airfoil data, and by use of a "coefficient of compensation" (dependent upon the location of the spindle axis), a representative spindle torque is obtained from this moment coefficient. Calculations are performed for three blade outlines and several nominal pitch ratios over a complete range of blade pitch settings.

When the present investigation was almost completed, the author discovered a method of calculating spindle torque devised by Van de Voorde.⁴ Van de Voorde presents a somewhat different approach to the problem of calculating the spindle torque than that of the present paper. The difference lies in the methods by which the calculations are performed. Van de Voorde calculates the hydrodynamic component of blade spindle torque by use of moment coefficients of standard NACA airfoil sections and centrifugal component of blade spindle torque by direct integration throughout the entire blade mass of the differential torque due to the centrifugal force on each element of blade mass.

In the present report, the optimum spindle axis (i.e., the radial axis about which the net torque due to the forces on the blade is zero) is determined by an iteration process in which the spindle torque is calculated about successive approximations to the optimum spindle axis.

The hydrodynamic component of blade spindle torque is calculated from the theoretical pressure distribution over the blade surface. The theoretical distribution over each blade section is obtained,^{5,6} and the distance from any point on the blade to the initial spindle axis is calculated from the blade geometry. The torque due to the pressure at each of a series of points along each section is then calculated, and this differential torque

distribution is numerically integrated, first along each blade section and then radially from root to tip, yielding the total hydrodynamic component of spindle torque.

A method of calculating the component of spindle torque due to the centrifugal force distribution over each blade section in terms of the moments of inertia of the blade sections is developed and used. Numerical integration of these differential spindle torques is performed radially from root to tip, yielding the centrifugal component of blade spindle torque.

GENERAL CONSIDERATIONS

The shape of the blade sections and the operating conditions of the blade fix the static pressure distribution and the centrifugal force distributions over each section. If a relationship approximating these distributions can be obtained from the operating conditions, then the method of approach to find the spindle torque is to integrate the force distribution over each section to find the resultant sectional torque, and then integrate these sectional spindle torques radially to find the spindle torque of the entire blade.

The hydrodynamic component of blade spindle torque is due to the chordwise static pressure distribution over the blade sections. The pressure distribution over a given airfoil section is a function of the angle of attack and the velocity of the fluid flowing over it. Thus for a propeller blade section, the pressure distribution is a function of the rotational velocity and the velocity of advance.

For an airfoil section, the "basic" pressure distribution; that is, the pressure distribution at ideal angle of attack,⁶ is a function of the section shape. The location of the center of this pressure distribution is slightly forward of the half-chord point for ordinary airfoil sections and is a function of the type of mean line used. For the uniform load line ($a = 1.0$ mean line), this center of pressure is very near the $1/2$ chord point and for mean lines with a calculated decrease in loading over the rear portion of the section (such as $a = 0.8$ mean line), this center of pressure is closer to the leading edge.⁷

The center of the "additional"⁶ pressure distribution; that is, pressure distribution due to angle of attack as measured from ideal angle of attack, is located at approximately 25 percent of the chord from the leading edge for all sections.^{6,7} The magnitude of this additional pressure distribution increases with increasing angles of attack and thus the center of pressure of the sections moves towards the quarter-chord point.

If the propeller is designed so that the sections operate at ideal angle of attack at design operation conditions, the pressure distribution over each section at design conditions will be the basic pressure distribution. As the advance coefficient decreases, the angle of attack becomes larger than design angle of attack, the additional pressure distribution increases in magnitude, and thus the center of pressure on the blade sections moves toward the quarter-chord point.

In the design of a propeller, the desired lift and hydrodynamic pitch angle at each radius are determined and then a section is selected to produce the desired lift in two-dimensional flow. However, if the propeller were built with the two-dimensional sections (same camber and angle of attack) laid along the helices, the propeller would be found from experience to be underpitched. The deficiency in pitch is due to "three-dimensional effects" in the propeller. These three-dimensional effects are compensated for in the design⁸ by applying correction factors to the camber and angle of attack at each section. With these correction factors, propellers are designed that develop the desired overall characteristics (thrust, pitch, cavitation suppression, etc.), but the lift distribution over each section is not necessarily the same as that over the two-dimensional section from which it was developed.

The actual lift distribution approximates the two-dimensional lift distribution only to the degree that the correction factors adjust the two-dimensional sections to the actual three-dimensional flow pattern along the blade section. In the present propeller design method, the corrections are based only on certain positions of the section, not continuously along the section. Hence, there is no way of theoretically determining the true three-dimensional lift distribution, and since no accurate experimental measurement of the actual pressure distribution

existing over a propeller blade has yet been made, it will be assumed that the lift distribution is to be the same as the two-dimensional lift distribution; that is, the correction factors applied in the propeller design are assumed to exactly adjust the section from the two-dimensional flow to three-dimensional flow.

In the calculation of the pressure distribution the blade sections are assumed to operate continually at the mean inflow velocity and angle of attack. But in actuality there is a wake variation which might, in the course of one revolution of the propeller, cause significant variation in the sectional angles of attack and hence in the pressure distribution and spindle torque. This could cause instantaneous spindle torques of much greater magnitude than those calculated at the mean flow conditions. Thus a reasonable factor of safety should be applied to any spindle torque calculations based upon mean flow conditions.

The centrifugal component of spindle torque arises from the centrifugal force acting radially outward on each increment of the blade mass of the rotating propeller. This component of spindle torque is due to the fact that, in general, the centrifugal force on each increment of blade mass has a component in the plane normal to the spindle axis.

Such design factors as the amount of blade rake and skew have a large effect upon the magnitude of the blade spindle torque as they offset the sections from the radial disc line. Large amounts of rake and skew are not generally used for controllable-pitch propellers due to clearance limitations over the range of pitch settings.

The spindle axis is usually radial, but for applications in which stern clearance is a problem at negative pitch settings the spindle axis is sometimes sloped in the aftward direction. For the purposes of calculations in this report the spindle axis is considered to be radial.

PROCEDURE

The primary problem considered is: given a blade design without the spindle located, find the location of the spindle so that the torque about the spindle axis due to the forces acting on the blade at design conditions

is zero. This "optimum" spindle axis location is determined by an iteration process. The torque is first calculated about a selected abstract axis and from the magnitude of this torque, a second abstract axis is determined which better approximates the optimum spindle axis location. Successively closer approximations to the optimum spindle axis location are made until the calculated torque about an axis is sufficiently near zero, this final axis being the determined optimum spindle axis location. Thus to obtain zero torque at design conditions the spindle should be located so that the actual axis of twist is this optimum spindle axis.

As a convenient starting point, the first abstract axis, called the "initial spindle axis" is taken as the projection of the pitch reference line in a plane normal to the propeller shaft and intersecting the pitch reference line in the section at the hub. This location is selected because the pitch reference line passes through the chord line of each blade section and serves as the reference line when delineating a screw propeller.⁹ Thus a relatively simple expression for the distance to this initial spindle axis from any point on the blade can readily be obtained from blade geometry. For subsequent abstract spindle axis locations, the expressions for distance are slightly more involved. For unskewed blades with maximum thickness at the section half-chord point, the pitch reference line passes through the half-chord point of each section; for skewed blades it usually, but not always, passes through the half-chord point of the section at the hub.⁹

A second type problem that can also be solved by the method of this report is: given a completely designed blade with the actual spindle axis location already fixed, find the spindle torque at design conditions. In this case, the spindle torque is directly calculated about the actual spindle axis.

HYDRODYNAMIC COMPONENT OF BLADE SPINDLE TORQUE

The hydrodynamic component of spindle torque is calculated from the pressure distribution over the blade surface. The pressure distribution may be determined by any available means since it is an input to the method of spindle torque calculation. For NACA sections the pressure

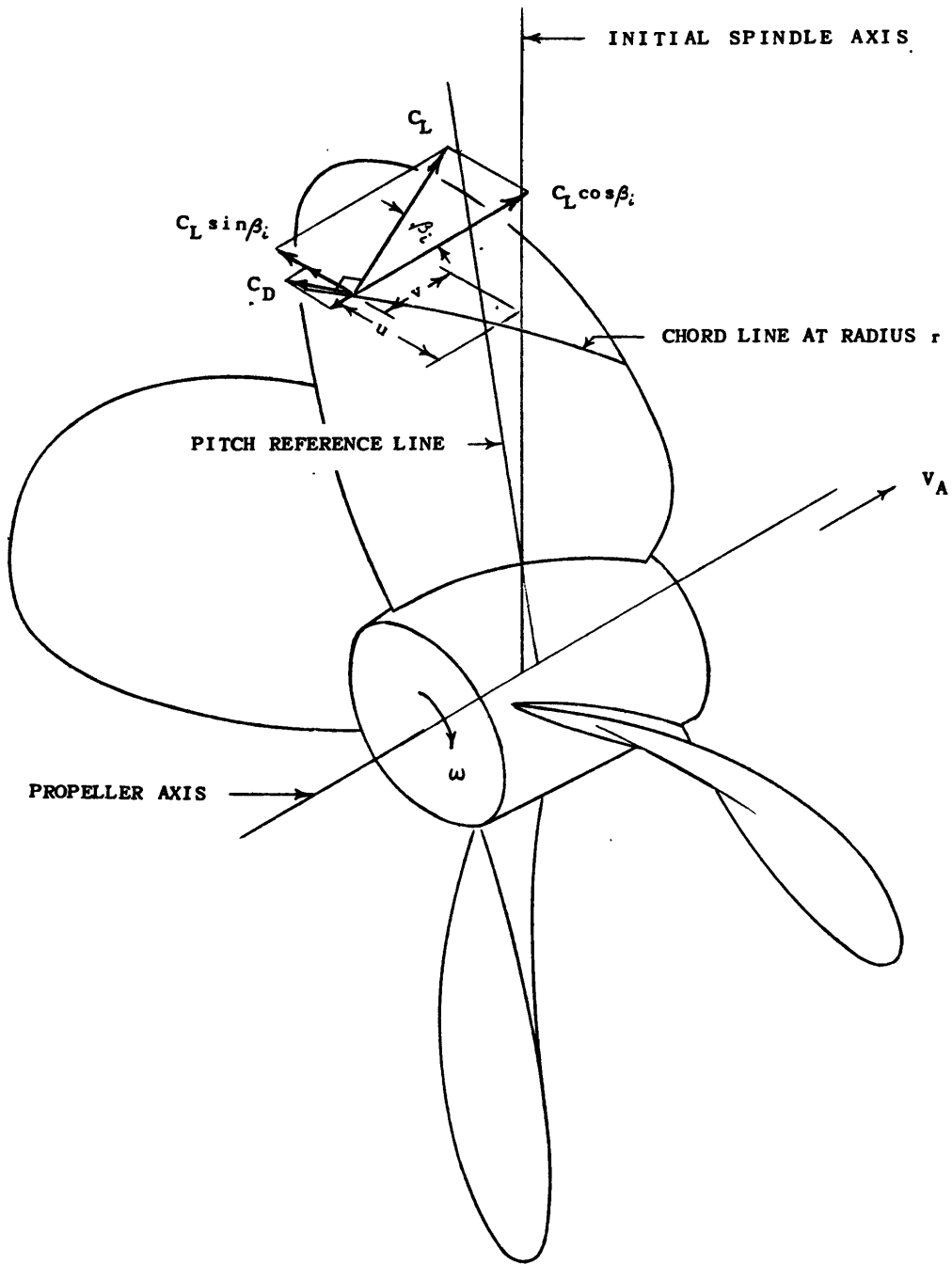


Figure 1 - Propeller Isometric Showing Hydrodynamic Forces

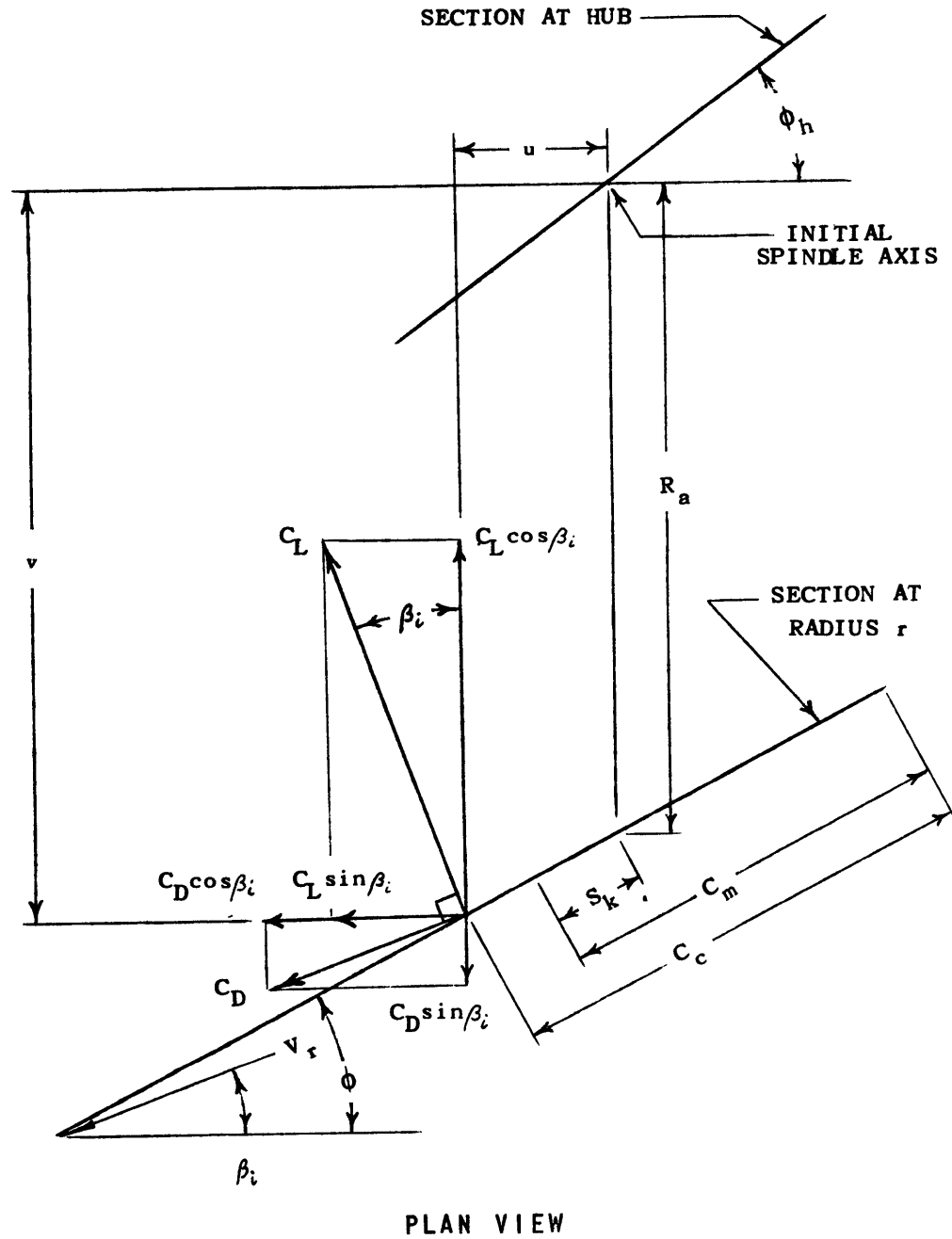


Figure 2 - Diagram of Hydrodynamic Forces and Distances to Initial Spindle Axis

distribution may be obtained quickly by the NACA approximate method.⁶ For such sections operating at ideal angle of attack, the pressure distribution and center of pressure are functions only of the type mean line and may be obtained directly from NACA data. For propellers with blade sections which are not of NACA type, the pressure distribution may be obtained by the AVA approximate method.⁵ This method may be used to calculate the pressure distribution over a body of arbitrary shape from the ordinates measured from the longest chord contained within the body and the operating angle of attack measured from this chord. The big disadvantage to this method is the tediousness of the work involved. Although the calculations are programmed for the UNIVAC high-speed computer,¹⁰ the ordinates must be measured on large-scale drawings (48" chord) for nonmathematical sections, and the pressure is obtained at inconvenient stations along the chord.

The lift and center of pressure of each blade section are obtained by integration of the pressure distribution (assumed to act normal to the velocity past the section, this velocity being the resultant inflow velocity to the section). The viscous drag coefficient is obtained from NACA data,⁶ and the drag force acts at the center of pressure in the direction of the velocity past the section. These lift and drag forces for each blade section are then decomposed into axial and tangential components. From the geometric characteristics of the blade, expressions are derived for the distances from the initial spindle axis to any axial and tangential force on the blade. The differential spindle torque due to the lift and drag on each blade section is then computed. These differential spindle torques are then radially integrated over the blade from root to tip, yielding the hydrodynamic component of spindle torque about the spindle axis. The differential hydrodynamic component of blade spindle torque at each radius is given by (see Figures 1 and 2):

$$Q'_h = \left[u(C_L \cos \beta_i - C_D \sin \beta_i) + v(C_L \sin \beta_i + C_D \cos \beta_i) \right] \frac{\rho}{2} V_r^2 l dr \quad [1]$$

where u and v , the tangential and axial components, respectively, of the distance from the initial spindle axis to the center of pressure are given by:

$$u = r \sin \left\{ \left[\frac{(C_m - C_c)}{100} \ell - S_K \right] \cos \phi \right\} \quad [2]$$

$$v = \left[\left(\frac{C_m - C_c}{100} \right) \ell - S_K \right] \sin \phi - R_a \quad [3]$$

For any given two-dimensional pressure distribution, the lift coefficient is:

$$C_L = \int_0^1 \left[(P/q)_{face} - (P/q)_{back} \right] dC_x \quad [4]$$

and the center of pressure (in percent chord from leading edge) is

$$C_c = \frac{1}{C_L} \int_0^1 \left[(P/q)_{face} - (P/q)_{back} \right] C_x dC_x \quad [5]$$

The drag coefficient, C_D , for standard airfoil sections may be obtained from experimental NACA data. At design conditions, the drag contribution to spindle torque will be very small, since the blade sections are generally designed to operate at ideal angle of attack where the drag coefficient is a minimum.

At off design conditions, the sections will not in general operate at design angle of attack, subsequently the drag coefficients may be many times greater than at design conditions and the spindle torque due to drag may become more significant.

The dynamic pressure, q , is based upon the resultant inflow velocity, V_r , hence:

$$q = \frac{1}{2} \rho V_r^2 \quad [6]$$

where

$$V_r = V_A \frac{\cos(\beta_i - \beta)}{\sin \beta} \quad \text{for free running propellers} \quad [7a]$$

$$V_r = V(1 - w_x) \frac{\cos(\beta_i - \beta)}{\sin \beta} \quad \text{for wake adapted propellers} \quad [7b]$$

From the propeller design calculations, the values of V_A , V , w_x , β_i , β , and α are known at design conditions. The only other needed quantities are geometric characteristics of the propeller (R_a , S_K , l , ϕ , C_m , R) which can easily be obtained from the propeller drawing or design calculations. The sign conventions are chosen so that spindle torques tending to rotate the blade toward larger forward pitch settings are positive. R_a is the offset of a section from the spindle axis due to rake and is thus the offset of the section from the propeller disc minus the offset of the section at the hub from the propeller disc. Hence for a propeller with a rake angle δ , the offset of the section at radius due to rake is simply

$$R_a = (r - r_h) \tan \delta \quad [8]$$

The hydrodynamic component of blade spindle torque is then obtained by integrating Equation 1 radially over the blade from root to tip:

$$Q_h = \frac{\rho}{2} R \int_{x_h}^l [u(C_L \cos \beta_i - C_D \sin \beta_i) + v(C_L \sin \beta_i + C_D \cos \beta_i)] V_r^2 dx \quad [9]$$

CENTRIFUGAL COMPONENT OF BLADE SPINDLE TORQUE

An expression is derived which expresses the differential centrifugal component of spindle torque at each radius in terms of the maximum and minimum moments of inertia of the blade sections, the blade sectional area, and the axial and tangential component distances from the spindle axis to the blade section centroid. The maximum and minimum sectional moments of inertia, the location of section centroids, and the sectional areas are estimated by the method in Reference 11. From the geometric characteristics of the blade, expressions are derived for the axial and tangential component

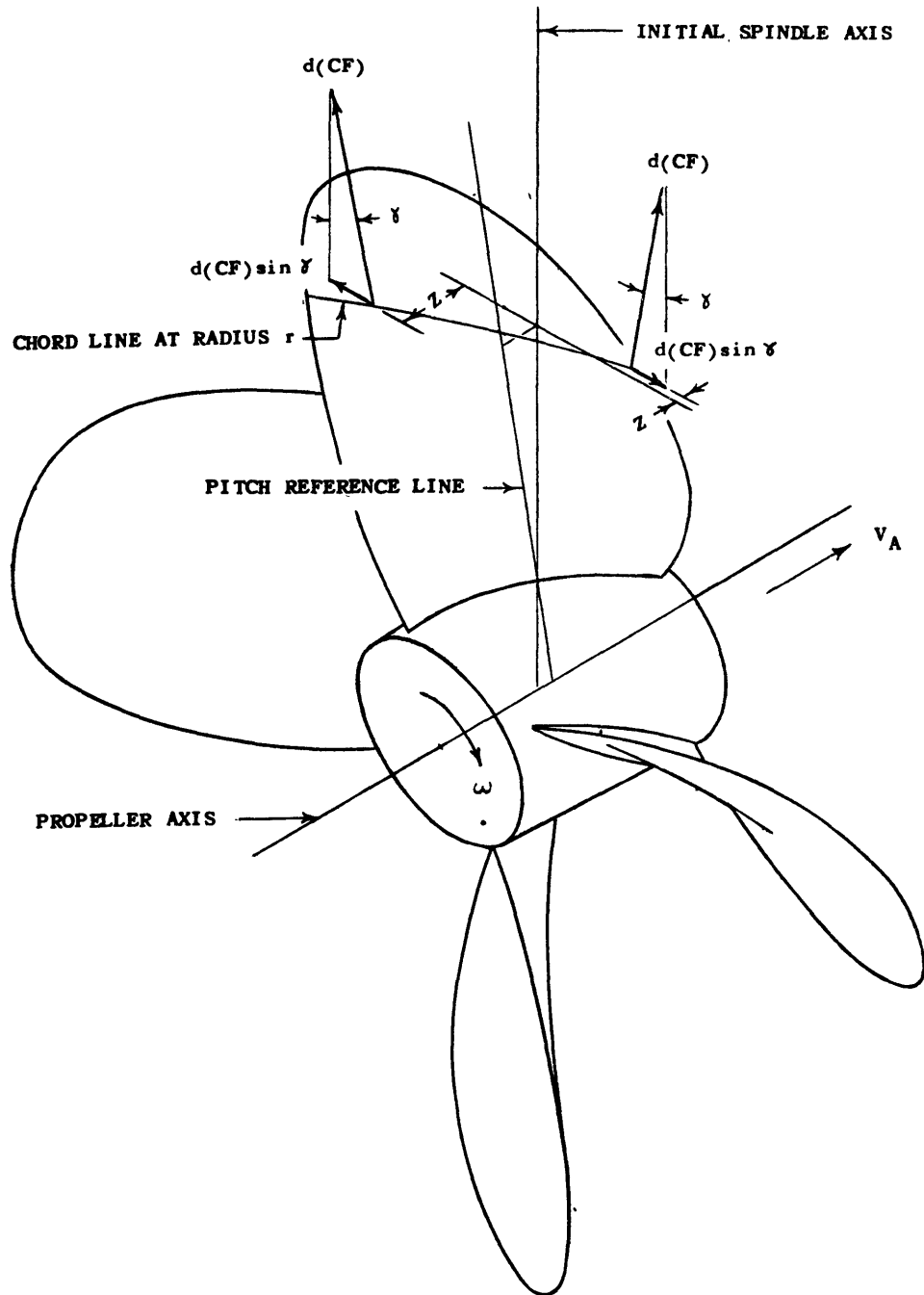


Figure 3 - Propeller Isometric Showing Centrifugal Forces

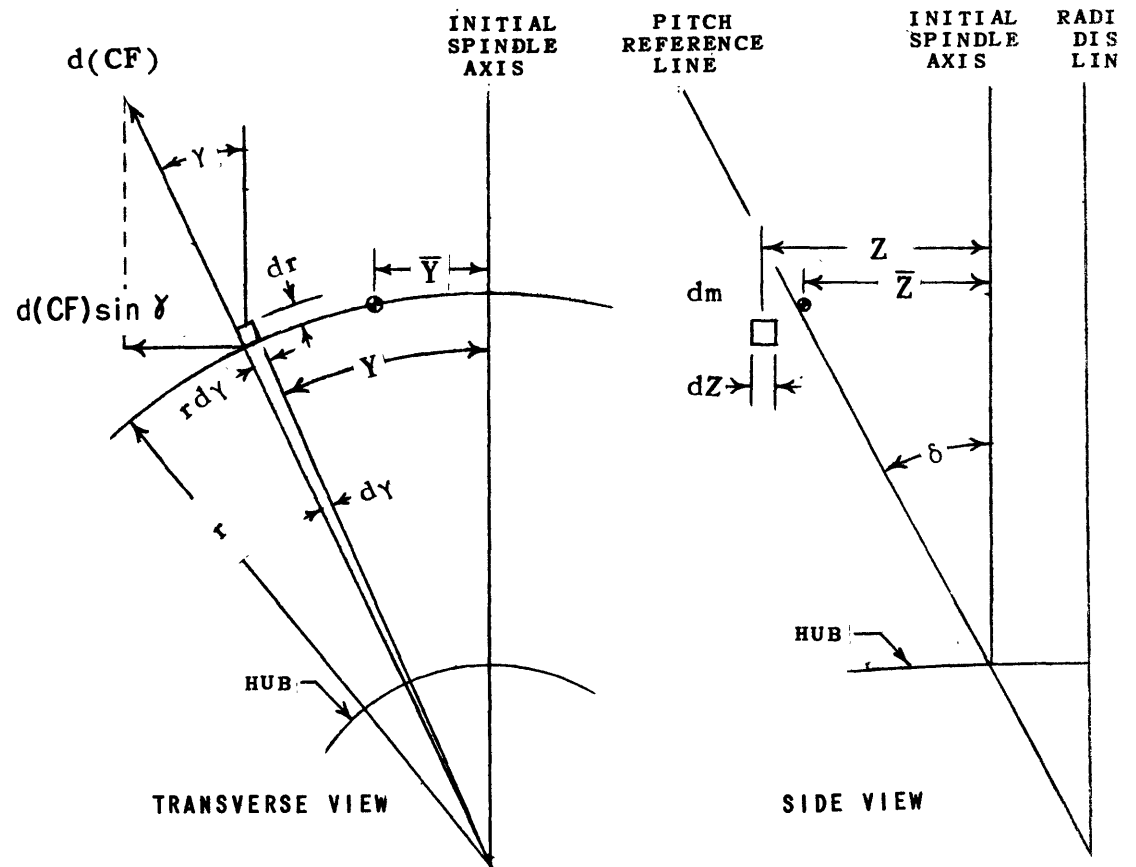
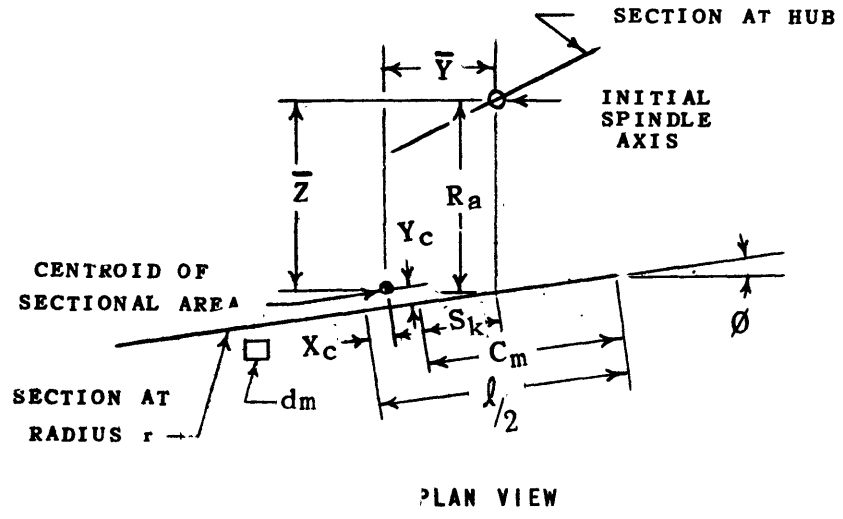


Figure 4 - Diagram of Centrifugal Forces and Distances to Initial Spindle Axis

distances from the spindle axis to the section centroids. Radial integration of these differential spindle torques yields the total centrifugal component of blade spindle torque.

The differential centrifugal component of spindle torque at each radius is approximated by:

$$Q'_c = -\rho_b \omega^2 \left[\frac{(I_{MAX} - I_{MIN}) \sin 2\phi}{2} + A \bar{Y} \bar{Z} \right] dr^{**} \quad [10]$$

The values of \bar{Y} and \bar{Z} in Equation 10 relative to the initial spindle axis are calculated from the geometric characteristics of the blade as follows:

$$\bar{Y} = r \sin \left\{ \frac{\left[\left(\frac{C_m - 50}{100} \right) l - S_K + X_c \right] \cos \phi - Y_c \sin \phi}{r} \right\} \quad [11]$$

$$\bar{Z} = \left[\left(\frac{C_m - 50}{100} \right) l - S_K + X_c \right] \sin \phi + Y_c \cos \phi - R_a \quad [12]$$

Reference 11 presents a simplified approximate method for calculating I_{max} , I_{min} , X_c , Y_c , and A for airfoil sections of the type commonly used in propeller design. For other type sections these values may be obtained by numerical integration. These sectional geometric characteristics in Equations 10, 11, and 12 refer to the projection of the developed sections in a plane normal to the spindle axis, but the values for the developed sections may be used as close approximations. The other geometric characteristics in Equations 10, 11, and 12 can readily be obtained from the propeller drawing. The total centrifugal blade spindle torque is then obtained by integration of Equation 10 over the blade from hub to tip:

$$Q_c = -\rho_b \omega^2 R \int_{x_h}^l \left[\frac{(I_{MAX} - I_{MIN}) \sin 2\phi}{2} + A \bar{Y} \bar{Z} \right] dx \quad [13]$$

* The derivation is presented in the appendix.

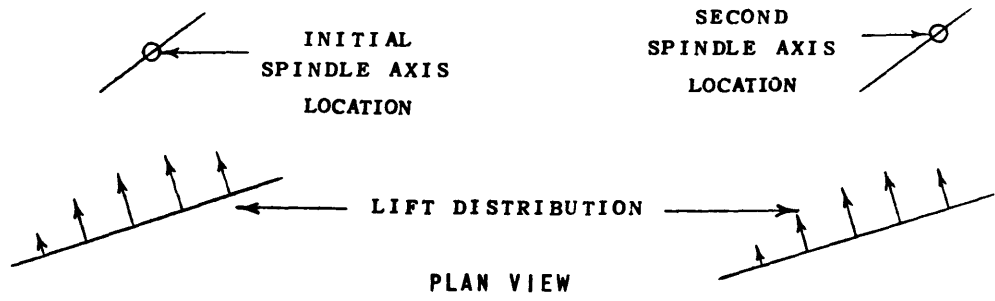


Figure 5 - Effect of Changed Spindle Axis Location on Hydrodynamic Blade Spindle Torque

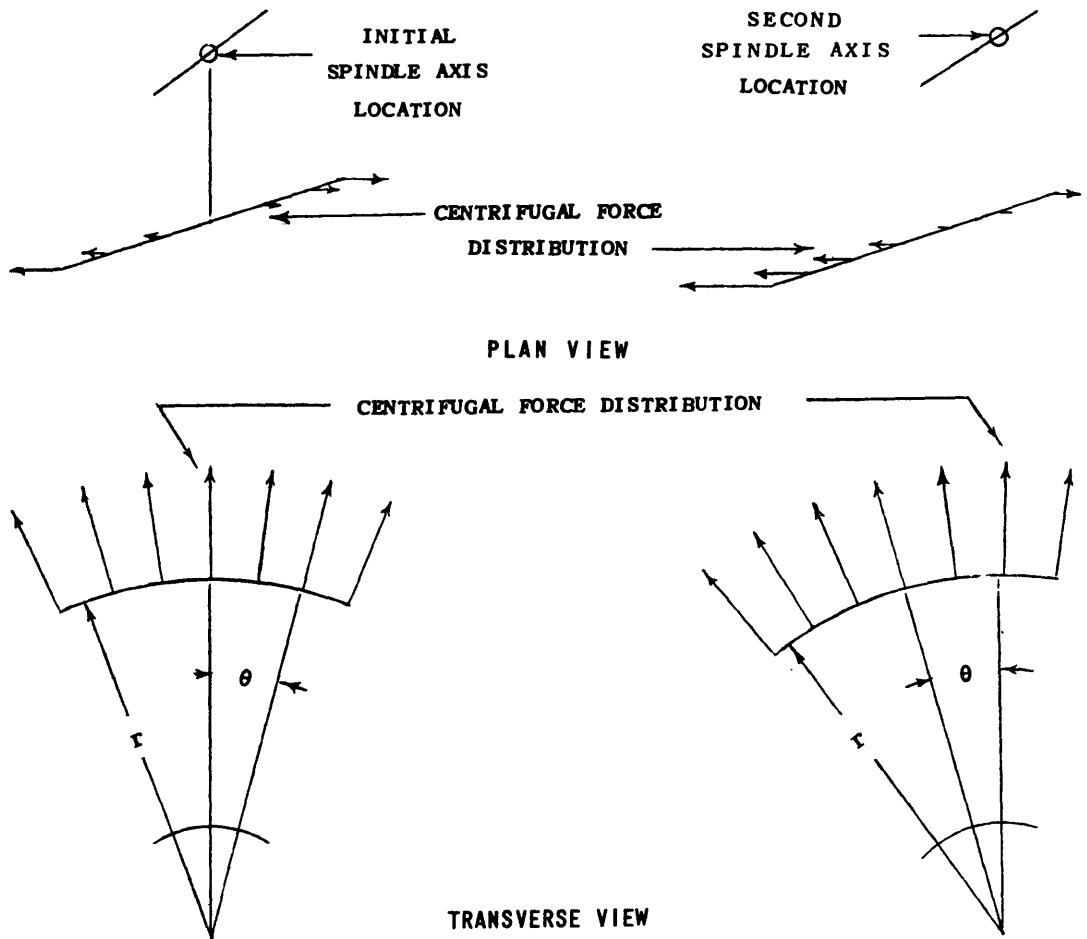


Figure 6 - Effect of Changed Spindle Axis Location on Centrifugal Blade Spindle Torque

CHANGED LOCATION OF SPINDLE AXIS

After the spindle torque has been calculated about the initial spindle axis, successive spindle axis locations are chosen and the spindle torque calculated about these axes in an effort to find the optimum spindle axis location. For convenience of calculation, these axes are taken radially through the chord of the section at the hub in a plane normal to the propeller axis. Thus all axes lie in the helical surface with pitch equal to that of the section at the hub at design pitch setting. Hence each axis can be regarded as rotated from the initial spindle axis by an angle, say Θ , about the propeller axis and shifted axially from the initial spindle axis, a distance of $r_h \Theta \tan \phi_h$.

The distances from the new spindle axis location to the components of forces on the blade are then:

(1) for the hydrodynamic blade spindle torque

$$u = r \sin \left\{ \left[\frac{(C_m - C_e)}{100} l - S_K \right] \cos \phi - \Theta \right\} \quad [14]$$

$$v = \left[\frac{(C_m - C_e)}{100} l - S_K \right] \sin \phi - R_a - r_h \Theta \tan \phi_h \quad [15]$$

(2) for the centrifugal blade spindle torque

$$\bar{y} = r \sin \left\{ \frac{\left[\frac{(C_m - 50)}{100} l - S_K + X_c \right] \cos \phi - Y_c \sin \phi}{r} - \Theta \right\} \quad [16]$$

$$\bar{z} = \left[\frac{(C_m - 50)}{100} l - S_K + X_c \right] \sin \phi + Y_c \cos \phi - R_a - r_h \Theta \tan \phi_h \quad [17]$$

Shifting the spindle axis towards the leading edge decreases the distance to the lift forces near the leading edge of the sections and increases the distance to the lift forces near the trailing edge of the sections. This has the effect of shifting the hydrodynamic spindle torque at design conditions toward negative values (tending towards lower positive pitch settings).

Since the direction of movement of the spindle axis is in a helical surface with pitch equal to that of the hub section, the spindle axis movement at each radius is in the general direction parallel to the section chord at that radius (see Figure 5). Due to the radial pitch variation, it is not actually parallel to the chord. The direction of spindle axis movement is nearly perpendicular to the lift forces, and thus movement is in the direction so as to have the maximum effect on the hydrodynamic blade spindle torque.

The centrifugal blade spindle torque is due to the component of centrifugal force in the plane normal to the spindle axis. When the spindle axis is moved, the distance to each increment of centrifugal force is changed by the axial distance which the spindle axis is moved (see Figure 6) and the components of centrifugal force in the plane normal to the spindle axis are slightly changed due to the angular movement of the spindle axis. The centrifugal component of spindle torque is thus expected to be much less sensitive to spindle axis location than is the hydrodynamic component of blade spindle torque.

Shifting the spindle axis towards the leading edge of the section at the hub at design pitch setting shifts both components of the section centroid offset from the spindle axis (\bar{Y} and \bar{Z}) towards negative values. For blades with after rake and positive skewback, both \bar{Y} and \bar{Z} are negative and shifting the spindle axis towards the leading edge increases the negative centrifugal component of spindle torque due to the offset centroid.

Thus, for a propeller with after rake and positive skewback, shifting the spindle axis towards the leading edge of the hub section will cause both the hydrodynamic and centrifugal components of spindle torque to change toward negative values and the change in the hydrodynamic component can be expected to be much greater than the change in centrifugal component.

OFF-DESIGN CONDITIONS

The method outlined in this report for calculating the spindle torque may be applied over the complete range of operating conditions (range of

loadings and pitch settings) provided that the pressure distribution and centrifugal force distribution are known at each condition. By the calculation of spindle torque about several spindle axis locations over the complete range of operating conditions, the spindle may be located so that the maximum spindle torque encountered under steady-state conditions will be as small as possible, regardless of the operating condition at which this maximum occurs.

The pressure distribution over a blade section is a function of the effective geometry of the section (thickness and camber) and the angle of attack at which the section is operating. At a given pitch setting, the geometry of each blade section remains unchanged but the angle of attack at which each section is operating varies as a function of the propeller advance. References 12 and 13 give approximate methods of calculating the section angles of attack at off-design advance. These methods are meant to apply to fixed pitch propellers but, for lack of a better method, they could be used for a controllable-pitch propeller at off-design pitch settings. As the blade is rotated about the spindle axis, the section of the blade cut by a cylindrical surface, whose axis coincides with the propeller axis, changes. Since for flow considerations, a blade section is considered as located at a constant radius, the effective blade sections change as the blade is rotated about the spindle axis. This complicates the problem of determining pressure distribution at off-design pitch settings. For a helical surface rotated about a radial line, Reference 14 gives a method of determining the deformation of this surface from a helical surface through two reference points of the original surface in its displaced position, at each radius in question.

The centrifugal component of spindle torque is a function of pitch setting and angular velocity but is not a function of blade loading. The effective change in blade section shape is small and its effect upon the centrifugal spindle torque is probably insignificant. If the effect of variation in section geometry is ignored, the centrifugal component of spindle torque varies only as a function of the propeller angular velocity and the pitch angle of each blade section; thus it can be calculated over the complete range of operating conditions without great difficulty.

For applications in which the pitch setting must be reversed rapidly for maneuvering purposes, the magnitude of the spindle torque during transient periods becomes important. Due to the complex and unsteady nature of the flow during emergency ahead and emergency astern operations, it is difficult to estimate the pressure distributions for these conditions. Experimental study seems to be the best approach to this problem.

EXAMPLE

An example calculation will now be performed to illustrate the procedure.

The calculations will be performed on the propeller from Appendix 2 of Reference 8 in which the design calculations for the propeller are performed. By referring to Reference 8, the reader can more directly see what quantities are available for the calculation of the spindle torque and how these quantities are obtained. This example propeller is a fixed-pitch propeller but at design conditions the geometry of a controllable-pitch propeller is almost identical to that of a fixed-pitch propeller designed to operate at the same conditions.

The design conditions for this propeller are as follows:

$$\begin{aligned}V &= 21 \text{ knots} \\P_e &= 13,000 \text{ ehp} \\P_s &= 17,500 \text{ shp} \\rpm &= 102 \\\omega &= 10.68 \text{ rad/sec} \\Diameter &= 21 \text{ ft} \\w_o &= 0.20 \\t &= 0.15\end{aligned}$$

The type blade section used in this propeller is the NACA 66 section with parabolic tail and a = 0.8 mean line.

The problem considered in this example is: given the fully designed propeller, find the location of the spindle so that the spindle torque will be a minimum at design conditions. As a good starting point, the torque will be calculated about the initial spindle axis.

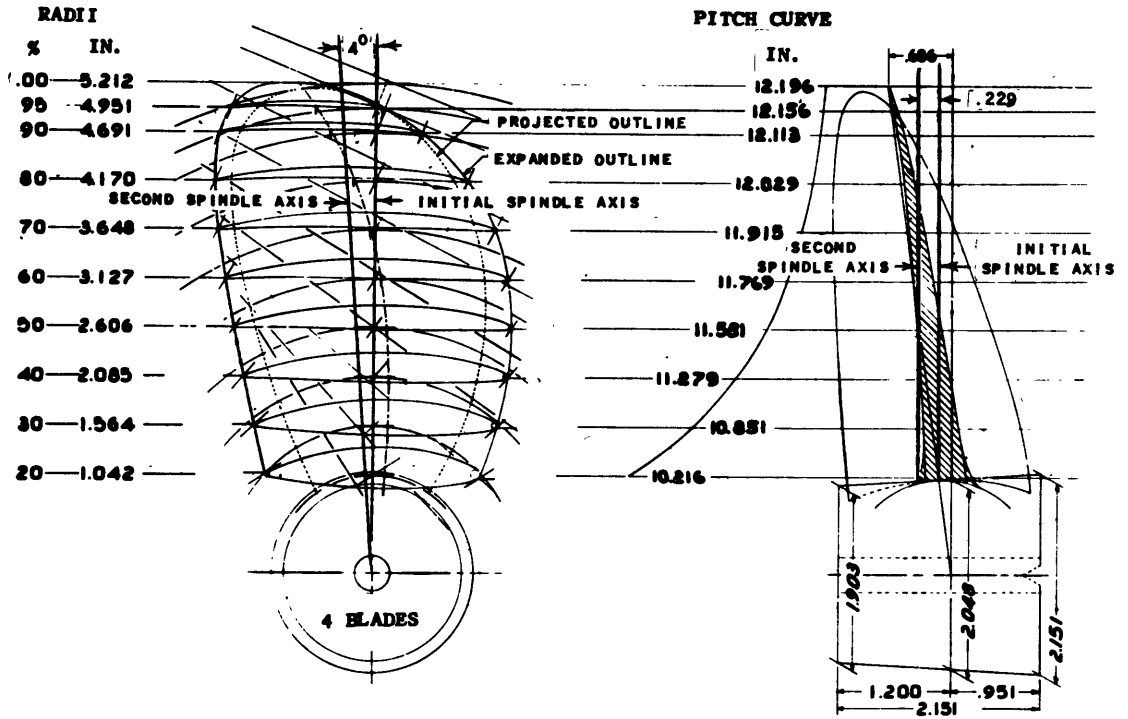


Figure 7 - Drawing of Example Propeller

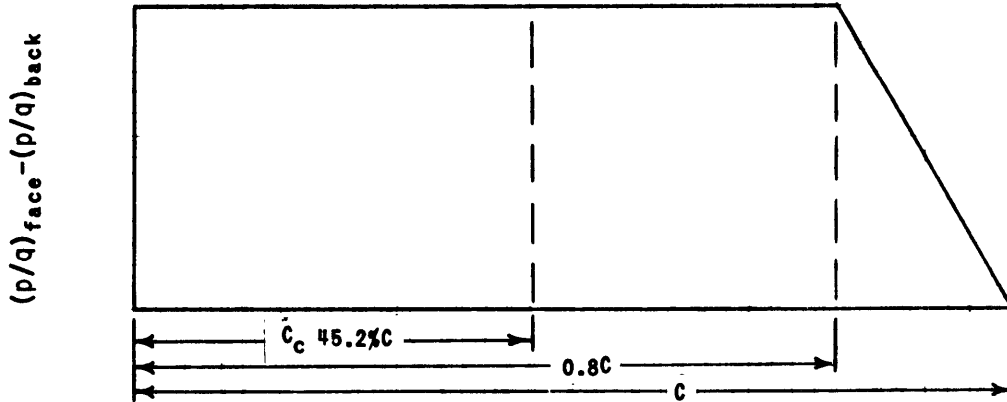


Figure 8 - Lift Distribution of $a=0.8$ Mean Line

A) HYDRODYNAMIC BLADE SPINDLE TORQUE

Properties of the additional blade sections at $x = .925, .95,$ and $.975$ were calculated in order to get a clearer picture of the radial spindle torque distribution in the region near the blade tip.

Step 1 - The center of pressure of the blade sections is determined. This propeller design is based upon shock free entry so that all the lift is produced by camber. Hence, assuming the propeller sections to operate at the conditions for which they are designed, the pressure distribution over each section is simply that produced by the NACA 0.8 mean line as given in the NACA data.⁶ Thus $C_c = 45.2$ for each section (0.8 mean line distribution and Equations 4 and 5).

Step 2 - The distances in the axial and tangential directions from the initial spindle axis to the section center of pressure are determined (columns 6 and 7).

Column (See page 23)

| | | |
|---|--------|--|
| 2 | 1 | from design calculation |
| 3 | S_K | from design calculations |
| 4 | ϕ | from design calculations |
| 5 | R_a | Equation (8); from design, $\mathcal{J} = 7.5^\circ$ |
| 6 | u | Equation (2); $C_m = 45$ for NACA 66 section |
| 7 | v | Equation (3) |

Step 3 - The section hydrodynamic component of blade spindle torque is then calculated

| | | |
|----|-------------------------|---|
| 8 | $(1-w_x)$ | from design calculations |
| 9 | $\cos(\beta_i - \beta)$ | from design calculations |
| 10 | $\sin\beta$ | from design calculations |
| 11 | V_r | Equation (7b) |
| 12 | C_L | from design calculations |
| 13 | $\cos\beta_i$ | from design calculations |
| 14 | $\sin\beta_i$ | from design calculations |
| 15 | Q'_h | Equation 1, $C_D = .008, \rho = 1.99 \frac{\text{lb-sec}^2}{\text{ft}^4}$ |

Step 4 - The hydrodynamic component of blade spindle torque is obtained by integration of Equation 1 from root to tip.

| | |
|----|--|
| 16 | Simpson's Multiplier |
| 17 | Simpson's Product = column 15 times column 16 |
| | $Q_h = \frac{\text{Radius}}{10} (\sum \text{column 17})$ |

| | 1 | 2 | 3 | 4 | 5 | 6 | 7 | 8 | 9 | 10 | 11 | 12 | 13 | 14 | 15 | 16 | 17 |
|----------------|-------|-------|--------|--------|-------|---------|-----------|-----------------------|-------------|----------|-------|---------------|---------------|-------------|-----------------------|--------------------|---------|
| x | 1 | S_k | ϕ | R_a | u | v | $(1-w_x)$ | $\cos(\beta-\beta_1)$ | $\sin\beta$ | V_r | C_L | $\cos\beta_1$ | $\sin\beta_1$ | Q_h' | SIMPSON'S MULTIPLIERS | SIMPSON'S PRODUCTS | |
| | (ft) | (ft) | (deg) | (ft) | (ft) | (ft) | | | | (ft/sec) | | | | (ft-lbs/ft) | | | |
| | 0.2 | 4.620 | -0.222 | 57.334 | 0 | 0.1143 | 0.1793 | 0.576 | 0.976 | 0.673 | 29.61 | 0.564 | 0.557 | 0.817 | +483.7 | 1/3 | +161 |
| | 0.3 | 5.229 | -0.300 | 47.844 | 0.138 | 0.1943 | 0.0768 | 0.656 | 0.983 | 0.568 | 40.23 | 0.506 | 0.704 | 0.710 | +809.1 | 4/3 | +1078 |
| | 0.4 | 5.691 | -0.316 | 40.730 | 0.276 | 0.2310 | -0.0775 | 0.712 | 0.988 | 0.490 | 50.90 | 0.435 | 0.786 | 0.619 | +829.2 | 2/3 | +553 |
| | 0.5 | 5.964 | -0.268 | 35.272 | 0.415 | 0.2090 | -0.2669 | 0.751 | 0.991 | 0.429 | 61.50 | 0.377 | 0.839 | 0.544 | +195.3 | 4/3 | +260 |
| $\frac{1}{10}$ | 0.6 | 6.069 | -0.134 | 30.921 | 0.553 | 0.1046 | -0.4897 | 0.779 | 0.994 | 0.380 | 72.24 | 0.329 | 0.875 | 0.482 | -1619 | 1/3+3/8 | -1147 |
| | 0.7 | 5.964 | +0.103 | 27.465 | 0.691 | -0.1021 | -0.7442 | 0.800 | 0.995 | 0.340 | 82.98 | 0.285 | 0.903 | 0.431 | -5015 | 9/8 | -5642 |
| | 0.8 | 5.460 | +0.466 | 24.665 | 0.829 | -0.4370 | -1.030 | 0.815 | 0.996 | 0.307 | 93.72 | 0.258 | 0.921 | 0.389 | -10,184 | 9/8 | -11,457 |
| | 0.9 | 4.389 | +0.963 | 22.343 | 0.968 | -0.8976 | -1.336 | 0.826 | 0.997 | 0.279 | 104.6 | 0.230 | 0.935 | 0.353 | -15,239 | 3/8+(1/3)(1/4) | -6984 |
| | 0.925 | 3.85 | +1.114 | 21.767 | 1.002 | -1.041 | -1.418 | 0.829 | 0.997 | 0.272 | 107.6 | 0.222 | 0.939 | 0.344 | -14,790 | (4/3)(1/4) | -4930 |
| | 0.950 | 3.22 | +1.276 | 21.281 | 1.037 | -1.191 | -1.502 | 0.832 | 0.997 | 0.267 | 110.2 | 0.218 | 0.942 | 0.337 | -14,160 | (2/3)(1/4) | -2360 |
| | 0.975 | 2.39 | +1.470 | 20.837 | 1.072 | -1.376 | -1.597 | 0.836 | 0.997 | 0.262 | 113.0 | 0.210 | 0.944 | 0.330 | -11,870 | (4/3)(1/4) | -3957 |
| | 1.000 | — | | | | | | | | | | | | 0 | (1/3)(1/4) | 0 | |

34,425

$$Q_h = \left(\frac{10.5}{10}\right)(34,425) = 36,146 \text{ ft-lbs.}$$

B) CENTRIFUGAL BLADE SPINDLE TORQUE

The NACA 66 section with parabolic tail and $a = 0.8$ mean line is used in this propeller. The equations for estimating the geometric characteristics of this section are given on page 358 of Reference 8. The following quantities are estimated by these equations:

$$A' = .963 (a t_x/1) l^2 \quad (a \text{ from Figure 24, Reference 8}) \quad [18]$$

$$x_{c_x} = l/2 - x_1$$

$$x_c = (.500 - .473 + .026 m_x/1) l \quad [19]$$

$$Y_c = -y_1$$

$$= +(.155 t_x/1 + 0.80) (m_x/1) l \quad [20]$$

$$I_{\min} = I_{x_0} \quad (\text{assuming the major axis of the section is parallel to the nose-tail line})$$

$$= .945 b (m_x/1)^2 + .04487 (t_x/1)^3 l^4 \quad [21]$$

(b from Figure 25, Reference 8)

$$I_{\max} = I_{y_0} \quad (\text{assuming the minor axis of the section is perpendicular to the nose-tail line})$$

$$= .914 (c) (t_x/1) l^4 \quad (c, \text{ from Figure 26, Reference 8}) \quad [22]$$

The geometric properties of each blade section are then calculated

as follows:

Column (See page 25)

| | | |
|----|------------|--------------------------------|
| 2 | $t_x/1$ | known from design calculations |
| 3 | $m_x/1$ | known from design calculations |
| 4 | 1 | known from design calculations |
| 5 | a | Figure 24, Reference 8 |
| 6 | b | Figure 25, Reference 8 |
| 7 | c | Figure 26, Reference 8 |
| 8 | A | Equation 18 |
| 9 | X_c | Equation 19 |
| 10 | Y_c | Equation 20 |
| 11 | I_{\min} | Equation 21 |
| 12 | I_{\max} | Equation 22 |

The location of the section centroid relative to the spindle axis is then found.

$$13 \quad \bar{Y} \quad \text{Equation 11}$$

$$14 \quad \bar{Z} \quad \text{Equation 12}$$

| 1 | 2 | 3 | 4 | 5 | 6 | 7 | 8 | 9 | 10 | 11 |
|-----|---------|---------|-------|--------|--------|---------|--------------------|--------|--------|--------------------|
| x | $t_x/1$ | $m_x/1$ | l | a | b | c | A | X_c | Y_c | I_{min} |
| | | | (ft) | | | | (ft ²) | (ft) | (ft) | (ft ⁴) |
| 0.2 | 0.1900 | 0.0349 | 4.620 | 0.7481 | 0.0097 | 0.04355 | 2.922 | 0.1294 | 0.1325 | 0.1375 |
| 0.3 | 0.1434 | 0.0360 | 5.229 | 0.7484 | 0.0065 | 0.04350 | 2.826 | 0.1464 | 0.1537 | 0.0994 |
| 0.4 | 0.1111 | 0.0367 | 5.691 | 0.7485 | 0.0046 | 0.04348 | 2.635 | 0.1593 | 0.1698 | 0.0692 |
| 0.5 | 0.0873 | 0.0370 | 5.964 | 0.7485 | 0.0036 | 0.04348 | 2.239 | 0.1670 | 0.1787 | 0.0416 |
| 0.6 | 0.0688 | 0.0363 | 6.069 | 0.7485 | 0.0026 | 0.04350 | 1.827 | 0.1699 | 0.1780 | 0.0231 |
| 0.7 | 0.0539 | 0.0345 | 5.964 | 0.7480 | 0.0022 | 0.04355 | 1.382 | 0.1670 | 0.1658 | 0.0115 |
| 0.8 | 0.0423 | 0.0320 | 5.460 | 0.7478 | 0.0016 | 0.04365 | 0.908 | 0.1526 | 0.1406 | 0.0042 |
| 0.9 | 0.0330 | 0.0291 | 4.389 | 0.7475 | 0.0013 | 0.04375 | 0.458 | 0.1229 | 0.1026 | 0.0010 |
| 1.0 | | | | | | | | | | |

| 12 | 13 | 14 | 15 | 16 | 17 | 18 | 19 | |
|--------------------|-----------|-----------|--|--------------------|-------------|-----------------------|--------------------|---------|
| I_{max} | \bar{Y} | \bar{Z} | $\frac{(I_{max} - I_{min}) \sin 2\phi}{2}$ | \overline{AYZ} | Q_c' | SIMPSON'S MULTIPLIERS | SIMPSON'S PRODUCTS | |
| (ft ⁴) | (ft) | (ft) | (ft ⁴) | (ft ⁴) | (ft-lbs/ft) | | | |
| 3.444 | -0.037 | +0.188 | +1.502 | -0.0203 | -2759 | 1 | -2759 | |
| 4.262 | +0.103 | +0.089 | +2.070 | +0.0026 | -3860 | 4 | -15,440 | |
| 4.778 | +0.035 | -0.022 | +2.328 | -0.0020 | -4330 | 2 | -8660 | |
| 4.389 | +0.008 | -0.190 | +2.050 | -0.0036 | -3809 | 4 | -15,236 | |
| 3.709 | -0.091 | -0.400 | +1.640 | +0.0662 | -3176 | 2 | -6352 | |
| 2.714 | -0.282 | -0.652 | +1.106 | +0.2536 | -2529 | 4 | -10,116 | |
| 1.581 | -0.594 | -0.948 | +0.598 | +0.5120 | -2066 | 2 | -4132 | |
| 0.489 | -1.064 | -1.294 | +0.344 | +0.6304 | -1813 | 4 | -7252 | |
| | | | | | 0 | 1 | 0 | |
| | | | | | | | | -69,947 |

$$Q_c = \left(\frac{1}{3}\right)\left(\frac{10.5}{10}\right)(69,947) = 24,481 \text{ ft-lbs.}$$

The spindle torque at each blade section is now computed

$$15 \quad \frac{(I_{\max} - I_{\min})}{2} \sin 2\phi$$

$$16 \quad A, \overline{YZ}$$

17 Q'_c - Equation 10. The blade material is naval brass

$$\rho_b = 525 \frac{\text{lb}}{\text{ft}^3}$$

The distribution of centrifugal spindle torque is next integrated over the blade from hub to tip to find the total centrifugal blade spindle torque.

18 Simpson's Multiplier

19 Simpson's Product - column 17 times column 18

C) LOCATION OF THE OPTIMUM SPINDLE AXIS

An approximation to the optimum spindle axis location is now made based upon blade geometry and the magnitude of the spindle torque about the initial spindle axis. The spindle torque about this new axis location is then calculated and, along with the previously calculated torque about the initial spindle axis location, is used to obtain a better estimation to the optimum spindle axis location. Successive calculations are performed until a sufficiently close approximation to the optimum location is obtained; that is, until the calculated spindle torque about an axis is sufficiently near zero.

In the example calculation, the torques about the arbitrary spindle axis are found to be:

$$Q_h = -36,146 \text{ ft-lb}$$

$$Q_c = -24,481 \text{ ft-lb}$$

$$Q_h + Q_c = -60,627 \text{ ft-lb}$$

Thus in an effort to find the optimum spindle axis location, the spindle axis must be shifted somewhat towards the rear of the blade. As an approximation to the optimum spindle axis location, the second spindle axis is taken radially through the hub section at an angle of 4 degrees towards the trailing edge, as measured from the initial spindle axis.

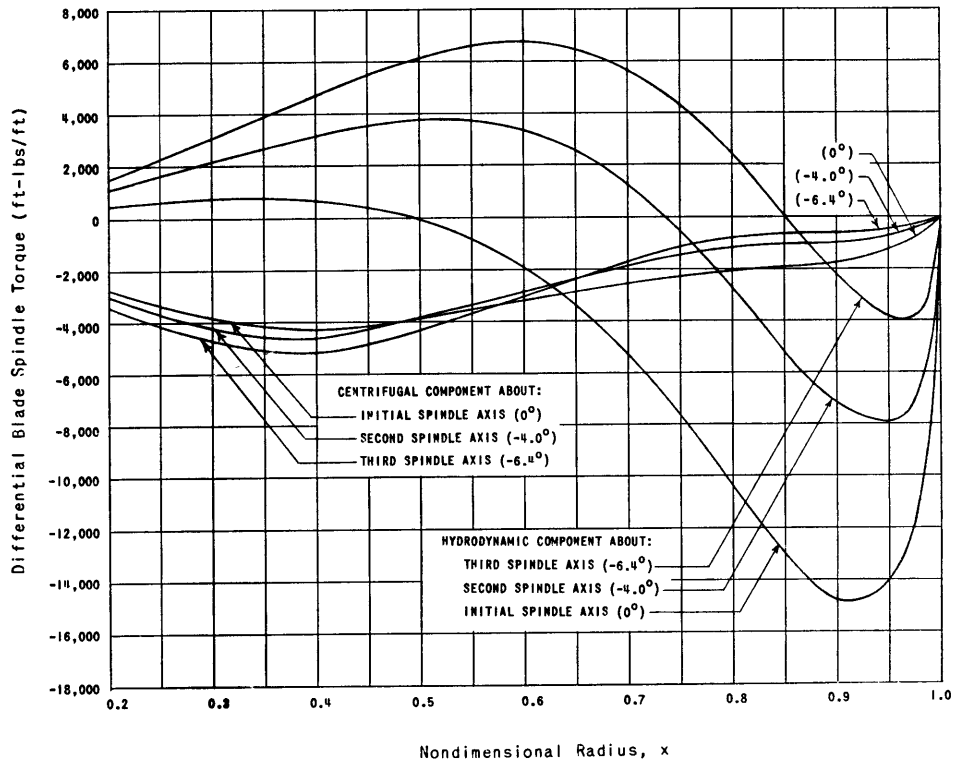


Figure 9 - Radial Distribution of Hydrodynamic and Centrifugal Components of Blade Spindle Torque for Example Propeller

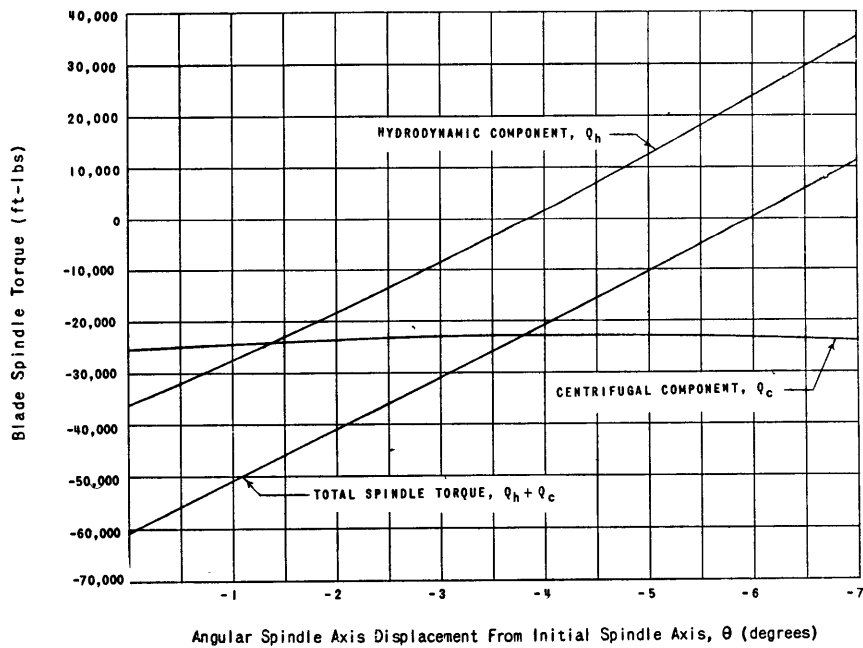


Figure 10 - Variation of Spindle Torque with Location of Spindle Axis for Example Propeller

This is a shift from the initial spindle axis of 5.9 percent of the hub section length.

The spindle torque about the new spindle axis is calculated by the same procedure as already shown for the previous spindle axis location. The only values that have changed are the distances to the spindle axis from various positions on the blade. For hydrodynamic blade spindle torque, u and v are calculated by Equations 14 and 15 respectively, and for centrifugal blade spindle torque, \bar{Y} and \bar{Z} are calculated by Equations 16 and 17, respectively.

The components of spindle torque about this second spindle axis location are calculated to be:

$$\begin{aligned}Q_n &= + 1675 \text{ ft-lb} \\Q_c &= -22,433 \text{ ft-lb} \\Q_n + Q_c &= -20,758 \text{ ft-lb}\end{aligned}$$

This smaller spindle torque of the same sign indicates that the shift is in the proper direction but is not great enough. A third spindle axis location is then taken at -6.4 degrees (9.4 percent of the hub section length) from the initial spindle axis. The components of spindle torque about this third spindle axis location are calculated to be:

$$\begin{aligned}Q_n &= 27,225 \text{ ft-lb} \\Q_c &= -23,317 \text{ ft-lb} \\Q_n + Q_c &= + 3,908 \text{ ft-lb}\end{aligned}$$

The total torque about this spindle axis is of reversed sign, hence this location is a little too far aft along the blade. By plotting spindle torque versus spindle axis location (see Figure 10), the optimum spindle axis location (zero spindle torque) is seen to be 6.0 degrees (8.8 percent hub section) aft the initial spindle axis.

CONCLUDING REMARKS

This report has outlined a workable method for calculating the spindle torque and for determining the optimum spindle axis location of a controllable pitch propeller at design conditions based upon two-dimensional chordwise pressure distributions.

Such design parameters as rake, skew, blade outline, type of blade sections, and pitch distribution are seen to influence the magnitude of the spindle torque. The results of the example indicate that the hydrodynamic component of blade spindle torque is much more sensitive to spindle axis location than is the centrifugal component.

The method of calculating the spindle torque outlined in this report can also be applied to off-design conditions provided that the pressure distribution at these conditions is known. The next logical step is to develop a method of approximating the pressure distribution at off-design conditions and by use of the method presented in this report, to investigate the effect of rake, skew, blade outline, type blade sections, and pitch distribution on spindle torque over a complete range of operating conditions. A subsequent report investigating the effect of these parameters over a range of operating conditions is planned. It is felt that such an investigation would greatly facilitate the design of controllable-pitch propellers for minimized spindle torque.

REFERENCES

1. Rupp, L.A., "Controllable-Pitch Propellers," Society of Naval Architects and Marine Engineers, Vol. 56, pp. 272-358 (1948)
2. Taylor, J.L., "The Variable-Pitch Marine Propeller," The Institution of Mechanical Engineers, Vol. 155, pp. 211-231 (1946)
3. Rusetskiy, A.A. and Favorskaia, A.V., "Gidrodinamicheskie Momenty Nalopastiakh Grebnykh Vintov Reguliruemogo Shage," Sudostroenie, No. 12, pp. 7-12 (1956)
4. Van de Voorde, C.B., "De Berekening van het Bladverstelkoppel Bij Verstelbare Schoeven en de Middelste Ter Verkleining van dit Koppel," Schip en Werf, Vol. 26, No. 17, pp. 505-509 (21 August 1959)
5. Riegels, F., "Über Die Berechnung der Druckverteilung von Profilen," Technische Berichte, Vol. 10 (1943); also David Taylor Model Basin Report Aero Memorandum 28 (March 1955)
6. Abbott, I.H., et al., "Summary of Airfoil Data," National Advisory Committee for Aeronautics Report No. 824 (1945)

7. Nonweiler, T., "The Design of Wing Sections," Aircraft Engineering, pp. 216-227 (July 1956)
8. Eckhardt, M.K. and Morgan, W.B., "A Propeller Design Method," Society of Naval Architects and Marine Engineers, Vol. 63, pp. 325-374, (1955)
9. "Explanatory Notes for Resistance and Propulsion Data Sheets," The Society of Naval Architects and Marine Engineers Technical and Research Bulletin No. 1-13 (1952)
10. Hecker, R., "Manual for Preparing and Interpreting Data of Propeller Problems Which Are Programmed for the High-Speed Computers at the David Taylor Model Basin," David Taylor Model Basin Report 1244 (Aug 1959)
11. Morgan, W.B., "An Approximate Method of Obtaining Stress in a Propeller Blade," David Taylor Model Basin Report 919 (Oct 1954)
12. Burrill, L.C., "Calculation of Marine Propeller Performance Characteristics," North East Coast Institute of Engineers and Shipbuilders, pp. 269-293 (1943-1944)
13. Kerwin, J.E., "Machine Computation of Marine Propeller Characteristics," International Shipbuilding Progress, Vol. 6, No. 60 (Aug 1959)
14. Lopkin, A.S. and Rusetskiy, A.A., "Towards the Calculations of the Hydrodynamic Characteristics of Variable Pitch Propellers," Bureau of Ships Translation, No. 726 (1960) [Translated from Sudostroenie, Vol. 11, No. 7, pp. 9-12, 1960]

APPENDIX

DERIVATION OF EXPRESSION FOR CENTRIFUGAL COMPONENT OF SPINDLE TORQUE

The centrifugal force on an element of blade mass, dm , is given by (see Figure 4):

$$dCF = r \omega^2 dm$$

$$dCF = \rho_b r \omega^2 (dZ)(dn)(r d\gamma)$$

The component of this centrifugal force in the plane normal to a radial axis is:

$$\sin \gamma dCF = \rho_b \omega^2 (dZ)(dn)(r d\gamma) r \sin \gamma$$

where γ is measured from the axis in question. Thus the spindle torque due to the centrifugal force on an element of blade mass is:

$$Q'_c = dCF \sin \gamma Z = \rho_b \omega^2 r \sin \gamma dn r d\gamma dZ$$

integrating over the sectional area:

$$Q'_c = \rho_b \omega^2 dn \int \int^A Z r \sin \gamma dZ r d\gamma \quad [a]$$

Evaluation of this integral over the blade sections would be a lengthy and tedious process. If $\sin \gamma$ is replaced by γ the integral takes the form of the product of inertia of the developed blade sections and thereby use can be made of the moments of inertia of the sections, which greatly reduces the amount of labor required to calculate the centrifugal component of blade spindle torque. Setting $\gamma = \sin \gamma$, Equation [a] becomes:

$$Q'_c = \rho_b \omega^2 dn \int \int^A Z r \gamma dZ r d\gamma \quad [b]$$

setting $Y = r \gamma$,

$$Q'_c = \rho_b \omega^2 dn \int \int^A Y Z dY dZ \quad [c]$$

But $\int \int^A Y Z dY dZ = I_{yz}$ [d]

where I_{yz} is the product of inertia of the developed sectional area about the spindle axis as the origin of the Y & Z axes. The product of

inertia about the spindle axis is now expressed in terms of the product of inertia about the section centroid as:

$$I_{YZ} = \bar{I}_{YZ} + A\bar{Y}\bar{Z} \quad [e]$$

The product of inertia about the section centroid is next expressed in terms of the maximum and minimum moments of inertia through the section centroid:

$$\bar{I}_{YZ} = \frac{(I_{MAX} - I_{MIN}) \sin 2\phi}{2} \quad [f]$$

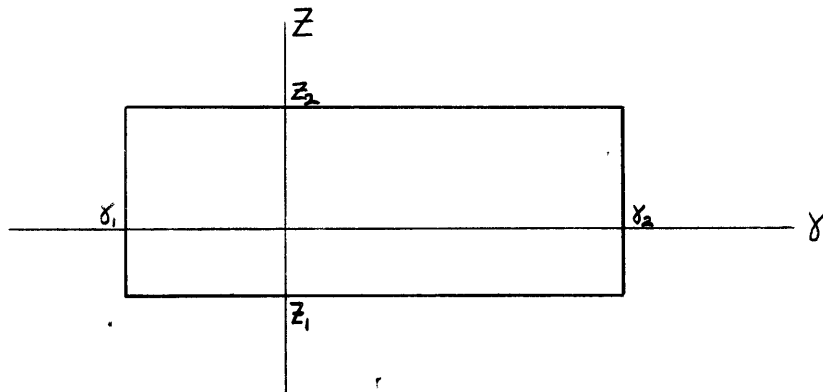
(This is under the assumption that the major and minor axes of the section are parallel and perpendicular, respectively, to the section chord.)

Substituting Equations [d], [e], and [f] into Equation [c] yields the desired relationship:

$$Q'_z = -\rho_b \omega^2 dr \left[\frac{(I_{MAX} - I_{MIN}) \sin 2\phi}{2} + A\bar{Y}\bar{Z} \right] \quad [10]$$

The negative sign is included so that the sign convention will agree with that of the hydrodynamic component of spindle torque; that is, positive spindle torques being those tending to twist the blade towards larger positive pitch settings.

In order to give an idea of the magnitude of the error introduced by the approximation $\gamma = \sin \gamma$, a comparison is made of Equations [a] and [b] (exact and approximate solutions, respectively) evaluated over a simple geometric section. Consider the rectangular section:



Exact solution (Equation [a]):

$$Q'_c = \rho_b \omega^2 r^2 dr \int_{\gamma_1}^{\gamma_2} \int_{z_1}^{z_2} Z \sin \gamma \, d\gamma \, dZ$$

$$Q'_c = k \int_{\gamma_1}^{\gamma_2} \int_{z_1}^{z_2} Z \sin \gamma \, d\gamma \, dZ = k \left(\frac{z_2^2 - z_1^2}{2} \right) (\cos \gamma_1 - \cos \gamma_2)$$

$$Q'_c = k \left(\frac{z_2^2 - z_1^2}{2} \right) \left(\sin^2 \frac{\gamma_2}{2} - \sin^2 \frac{\gamma_1}{2} \right)$$

Approximate solution (Equation [b]):

$$Q'_c = \rho_b \omega^2 r^2 dr \int_{\gamma_1}^{\gamma_2} \int_{z_1}^{z_2} Z \gamma \, dZ \, d\gamma$$

$$Q'_c = k \left(\frac{z_2^2 - z_1^2}{2} \right) \left(\frac{\gamma_2^2 - \gamma_1^2}{2} \right)$$

$$\frac{\text{Exact } Q'_c}{\text{Approx } Q'_c} = \frac{k \left(\frac{z_2^2 - z_1^2}{2} \right) \left(\sin^2 \frac{\gamma_2}{2} - \sin^2 \frac{\gamma_1}{2} \right) 2}{k \left(\frac{z_2^2 - z_1^2}{2} \right) \left(\frac{\gamma_2^2 - \gamma_1^2}{2} \right)}$$

$$\frac{\text{Exact } Q'_c}{\text{Approx } Q'_c} = \frac{\sin^2 \frac{\gamma_2}{2} - \sin^2 \frac{\gamma_1}{2}}{\left(\frac{\gamma_2}{2} \right)^2 - \left(\frac{\gamma_1}{2} \right)^2}$$

$$\lim_{\gamma_2 \rightarrow \gamma_1} \left[\frac{\sin^2 \frac{\gamma_2}{2} - \sin^2 \frac{\gamma_1}{2}}{\left(\frac{\gamma_2}{2} \right)^2 - \left(\frac{\gamma_1}{2} \right)^2} \right] = \frac{\sin \gamma_1}{\gamma_1}$$

Table of $\frac{\text{Exact } Q'_c}{\text{Approximate } Q'_c}$ for rectangular section as function of γ_1 and γ_2

| | | γ_1 , degrees | | | | | | | | | |
|----------------------|----------|----------------------|----------|----------|----------|----------|----------|----------|----------|----------|----------|
| | | 0 | ± 10 | ± 20 | ± 30 | ± 40 | ± 50 | ± 60 | ± 70 | ± 80 | ± 90 |
| γ_2 , degrees | 0 | 1.00 | 1.00 | 0.99 | 0.98 | 0.96 | 0.94 | 0.91 | 0.88 | 0.85 | 0.81 |
| | ± 10 | | 0.99 | 0.99 | 0.97 | 0.96 | 0.93 | 0.91 | 0.88 | 0.85 | 0.81 |
| | ± 20 | | | 0.98 | 0.96 | 0.95 | 0.92 | 0.90 | 0.87 | 0.84 | 0.81 |
| | ± 30 | | | | 0.96 | 0.94 | 0.91 | 0.89 | 0.86 | 0.83 | 0.79 |
| | ± 40 | | | | | 0.92 | 0.89 | 0.87 | 0.84 | 0.81 | 0.77 |
| | ± 50 | | | | | | 0.88 | 0.85 | 0.83 | 0.80 | 0.75 |
| | ± 60 | | | | | | | 0.83 | 0.81 | 0.78 | 0.73 |
| | ± 70 | | | | | | | | 0.77 | 0.75 | 0.70 |
| | ± 80 | | | | | | | | | 0.71 | 0.67 |
| | ± 90 | | | | | | | | | | 0.64 |

These errors are, of course, larger than would occur for a blade section with similar γ_1 and γ_2 , since the thickness of a usual blade section is reduced where γ is largest.

On the propeller used in the example calculation of this report, a maximum γ of 40° occurs (at the section at the hub). At greater radii where the centrifugal force is larger, the maximum sectional γ 's are smaller. This indicates that the approximation $\gamma = \sin \gamma$ introduces an error of less than 5% in the centrifugal component of spindle torque for this propeller. The value of γ on controllable-pitch propellers as a rule is not exceedingly large, since the blade width is limited by interferences between the blades at various pitch settings and greatly skewed blades are not generally used. For any particular propeller, the reader may decide whether or not the approximation is close enough for his purpose. If not, graphical or numerical integration of Equation [a] may be used to obtain a more accurate solution.

INITIAL DISTRIBUTION

Copies

10 CHBUSHIPS
 1 Tech Asst (Code 106)
 1 Lab Mgt (Code 320)
 3 Tech Info Br (Code 335)
 1 Prelim Des Br (Code 420)
 2 Mach Sci & Res (Code 436)
 2 Prop, Shaft, & Brng (Code 644)

2 CHONR
 1 Fluid Dynamics Br (Code 438)
 1 Library (Code 740)

1 CDR, USNOTS, Pasadena Annex

1 DIR, USNRL

1 SUPT, USNAVPGSCOL

10 ASTIA

1 ADMIN, Maritime Admin

1 O in C, PGSCOL, Webb

1 HD, Dept NAME, MIT

1 DIR ORL, Penn State

1 HD, Dept of NAME, Univ of Mich

1 DIR, Inst of Engin Res, Univ of Calif, Berkeley 4, Calif

1 DIR, Davidson Lab, SIT, Hoboken, N.J.

1 Peter P. Gillis, Div of Engin, Brown Univ, Providence 12, R.I.

1 J.E. Kerwin, Dept NAME, MIT

1 SNAME, 74 Trinity Place, New York 6, N.Y.

1 Gibbs & Cox Inc.

1 NNS & DD Co

1 Central Tech Div, Bethlehem Steel, Ship Div, Quincey, Mass

1 Dr. Benjamin Posniak, Karman Aircraft Corp, Bloomfield, Conn.

1 Dr. H.W. Lerbs, DIR, Hamburgische Schiffbau-Versuchsanstalt,
 Bramfelder Strasse 164, Hamburg, Germany

1 SUPT, Ship Div, Natl Phys Lab, Teddington, Middlesex, England

1 Prof. L.C. Burrill, HD, Dept of Naval Architecture, Kings College,
 Newcastle-upon-Tyne, England

- 1 DIR, Nederlandsch Scheepsbouwkundig Proefstation, Wageningen,
The Netherlands
- 1 Dr. Eng. Tatsumi Izubuchi, Secretary, Shipbuilding Research
Association of Japan, Tokyo, Japan
- 1 HD, Dept of Naval Arch, University of Naples, Naples, Italy
- 1 Director Prof. Dr. Ing. Weinblum, Institute fur Schiffbau,
Lammersieth 90, Hamburg, Germany

DEC 02 1982